Remote Sensing and GIS-Based Landslide Hazard Zonation: A Case Study from Western Ghats, Kerala, India

Arunkumar K.S.♥ and Mufeeda C.T.

Department of PG Studies & Research in Geology, MES Ponnani College, South Ponnani, Malappuram, India
♥Correspondence: ksarunenv@gmail.com

Article history: submitted: December 4, 2025; accepted: March 30, 2026; available online: April 23, 2026

Abstract

Background: Landslides are among the most destructive natural hazards in the hilly regions of Kerala, causing severe environmental and socio-economic damage. Nilambur Taluk in Malappuram District, located along the Western Ghats, has experienced frequent landslide events, particularly during the extreme rainfall events of August 2018 and 2019. **Aim:** This study aims to delineate landslide hazard zones in Nilambur Taluk using a GIS-based weighted overlay approach to support risk reduction and spatial planning. **Methods:** A landslide hazard zonation (LHZ) map was developed using an inverse ranking-based weighted overlay method. Multiple thematic layers—including slope, rainfall distribution, lineament density, drainage density, slope aspect, geology, land use/land cover (LULC), NDVI, elevation, distance from drainage, distance from road networks, and soil—were derived from Survey of India (SoI) toposheets and 2019 Landsat imagery. These layers were integrated within a GIS environment (ArcGIS 10.1). Each parameter was assigned a relative weight based on its contribution to landslide susceptibility, while classes within each layer were ranked on a scale of 0–5. **Conclusion:** The resulting LHZ map classifies the study area into five hazard categories: stable (5.8%), moderately stable (32.3%), moderately unstable (39%), highly unstable (22%), and critical (0.92%). Validation through field observations and geospatial analysis confirms that high and critical hazard zones are strongly associated with intense rainfall, steep slopes, high lineament density, and active erosional processes. The generated hazard zonation map serves as an effective tool for landslide risk mitigation, informed land-use planning, and sustainable geo-environmental management in Nilambur Taluk.

Keywords: landslides; hazard zonation; Nilambur; weighed overlay method (WOM)

1. Introduction

Landslides represent one of the most destructive natural hazards in mountainous regions, causing extensive loss of life, damage to property, and disruption to infrastructure worldwide (Froude & Petley, 2018). Global disaster statistics indicate that rainfall-induced landslides account for thousands of fatalities annually, along with significant economic losses. Between 2000 and 2020, more than 55,000 landslide-related deaths were reported globally, particularly concentrated in monsoon-dominated terrains (Froude & Petley, 2018).

The Western Ghats of southern India form a major orographic feature that exerts strong control over regional climatic gradients, separating the humid western coastal belt from the semi-arid inland regions (Gunnell & Fleitout, 2000). Nearly 80% of rainfall-triggered landslides in India occur during the southwest monsoon season (June–September), when prolonged or extreme precipitation elevates pore-water pressure and destabilizes slopes (Chen & Wang, 2007;Martha et al., 2019). Kerala, located on the windward side of the Western Ghats, has experienced a notable increase in landslide incidents in recent years. The extreme rainfall event of August 2018 alone triggered more than 5,200 landslides across the state (Martha et al. 2019), followed by widespread failures during the 2019 and 2020 monsoons.

This work is licensed under a Creative Commons Attribution-ShareAlike 4.0 International License. Copyright © 2026 the authors

Several studies have investigated landslide susceptibility in different parts of the Western Ghats and Kerala using geospatial techniques. For instance, GIS-based landslide susceptibility mapping has been conducted in districts such as Idukki, Wayanad, and Kottayam using statistical and multi-criteria decision-making approaches (Ajin et al., 2014; Prasannakumar & Vijith, 2012; Jishnusachidanandhan & Ajith, 2015). These studies demonstrate the effectiveness of remote sensing and GIS techniques in identifying landslide-prone areas across the Western Ghats. However, most existing studies are concentrated in a few well-documented districts, and several vulnerable regions remain insufficiently investigated.

Although high-intensity rainfall is the primary trigger for slope failures in Kerala (Kuriakose et al., 2009; Nima et al., 2025), several anthropogenic factors—including deforestation, changes in land-use/land-cover patterns, unregulated slope modification, quarrying, and soil piping—significantly exacerbate slope instability. Kerala is also one of the most densely populated states in India, and increasing developmental pressure on mountain slopes has contributed to land degradation and a higher likelihood of hazard occurrence.

Despite being one of the most landslide-prone landscapes along the Western Ghats, Nilambur Taluk in Malappuram District has received comparatively limited scientific attention in terms of landslide hazard assessment. Previous investigations in the broader Kerala region have largely focused on district-scale susceptibility mapping, while detailed hazard zonation specifically for Nilambur remains scarce. In particular, the region lacks (i) a systematic landslide inventory database, (ii) integrated analysis combining multiple environmental conditioning factors, and (iii) validation of susceptibility results using field-based observations. These limitations restrict the development of reliable spatial planning tools for landslide risk reduction in Nilambur Taluk (Amrutha et al., 2026; Badapalli et al., 2025; Md. Motiur Rahman et al., 2025).

Remote sensing and GIS-based approaches provide effective tools for analysing terrain parameters and delineating susceptible zones in inaccessible or rugged terrain. Such approaches allow the integration of multiple conditioning factors—including topographic, geological, hydrological, and land-use variables within a spatial modelling framework to generate landslide hazard zonation maps (Doukanari et al., 2025).

In this context, the present study aims to produce the first comprehensive landslide hazard zonation (LHZ) map for Nilambur Taluk using a GIS-based weighted overlay method with an inverse ranking scheme. The study integrates thirteen conditioning parameters derived from multi-source geospatial datasets, including DEM-based terrain attributes, geological and hydrological variables, land-use patterns, and rainfall distribution. Furthermore, the resulting hazard zonation map is validated using historical landslide inventory data and field observations. This integrated methodological and spatial approach provides a more robust understanding of landslide susceptibility in Nilambur and contributes to improved disaster risk reduction, land-use planning, and sustainable geoenvironmental management in the region. This study aims to delineate landslide hazard zones in Nilambur Taluk using a GIS-based weighted overlay approach to support risk reduction and spatial planning

2. Methods

The study area, Nilambur Taluk in Malappuram District, is located along the western foothills of the Western Ghats between 11°16′37″–11°17′00″ N and 76°13′33″–76°15′00″ E (Fig. 1), covering an area of approximately 1,397 km^2. The region is bounded by the

Nilgiri Hills to the east, Eranadu Taluk to the west, Mannarkad and Perinthalmanna Taluks of Palakkad District to the south, and Kozhikode District to the north. Nilambur consists of 19 revenue villages and hosts a population of about 574,059. The area forms part of the humid tropical belt of Kerala and experiences a monsoon-dominated

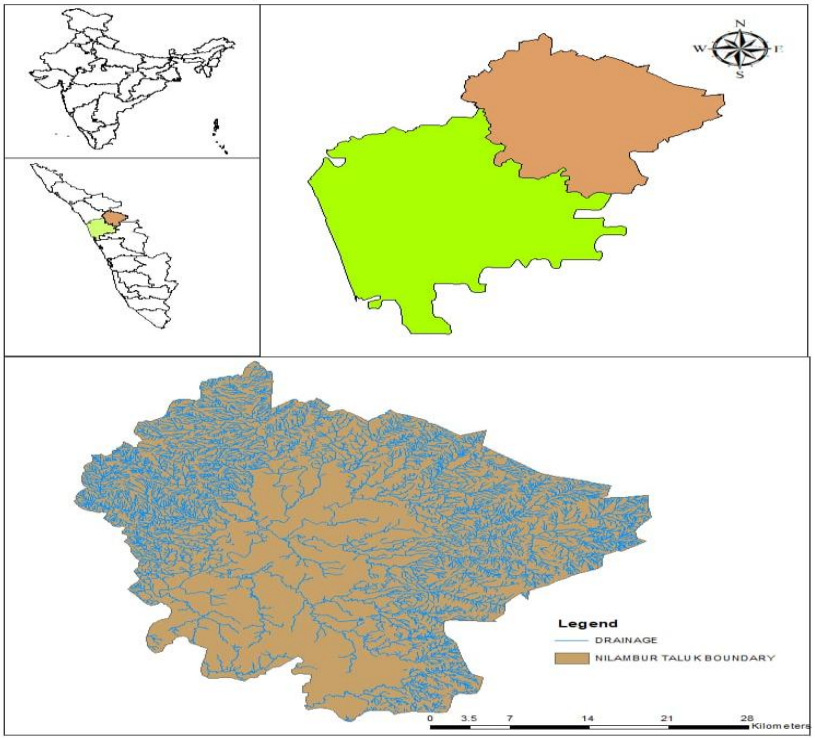

Figure 1. Location map of study area

Climate, with distinct southwest (June–September) and northeast (October–December) monsoon seasons. The southwest monsoon contributes nearly 80% of the annual rainfall, with the region receiving an average of ~3000 mm and mean annual temperature of about 27 °C (IMD 2020; Rajendran et al. 2022). The topography is predominantly undulating, characteristic of the midland and highland geomorphic zones of the Western Ghats.

Geologically, Nilambur is dominated by Precambrian crystalline rocks belonging to the Charnockite Group and Peninsular Gneissic Complex (Olade, 2025). The Charnockite Group—comprising charnockite, charnockite gneiss, granitic gneiss and hornblende–biotite gneiss—constitutes the major lithological unit in the region. Other associated lithologies occurring in varying proportions include banded magnetite quartzite, pyroxene granulite, amphibolite, hornblende granulite and pyroxenite. The eastern sector includes migmatitic rocks represented by biotite–hornblende gneiss and quartzofeldspathic gneiss. Pegmatite and quartz veins form the dominant acidic intrusives, whereas dolerite and gabbro occur as basic intrusive bodies.

Lateritisation is extensive across the midland zones, with laterite profiles exceeding 10 m thickness in several localities (Pichamuthu, 1976; Shafi & Khan, 2025). Isolated remnants of Neogene Warkalli sediments occur in parts of the region, while Quaternary unconsolidated fluvial and colluvial deposits are confined to valley floors and low-lying areas (Sreekumar & Arish, 2017). The geological and geomorphic diversity of the area,

combined with intense monsoonal rainfall, contributes significantly to its high susceptibility to landslides and related slope instability processes.

The study area is covered by Survey of India (SOI) Toposheets 58A/3 and 58A/7 (1:50,000 scale). The toposheets were georeferenced to the Universal Transverse Mercator (UTM) coordinate system using the WGS 84 datum, employing the nearest-neighbour resampling technique. A range of thematic layers—including slope, elevation, aspect, land-use/land-cover (LULC), lineament density, drainage density, soil type, distance from road network, distance from drainage, distance from lineaments, geology, NDVI, and rainfall distribution—were generated for the preparation of the landslide hazard zonation (LHZ) map.

All spatial dataset preparation, processing, and analysis were performed using ArcGIS 10.3 (ESRI, Redlands, USA), while image classification and spectral analysis were carried out using ERDAS Imagine 9.2. LULC and NDVI were derived from Landsat-8 OLI imagery (2019), obtained from the USGS Earth Explorer platform (https://earthexplorer.usgs.gov/). A supervised classification was performed in ERDAS Imagine. Slope, aspect, and elevation maps were extracted from CartoDEM (30-m resolution) using the Spatial Analyst and 3D Analyst extensions in ArcGIS. Geology, drainage density, and soil maps were digitized from Geological Survey of India (GSI) maps. Lineaments were digitized from the Bhuvan Web Map interface, while road networks were extracted from Google Earth and processed in ArcGIS. Rainfall distribution was modelled using the inverse distance weighting (IDW) interpolation technique in ArcGIS, utilizing mean daily rainfall data obtained from the India Meteorological Department (IMD). A summary of the datasets and their sources is presented in Table 1.

Table 1. Data and sources

SL NO	DATA LAYERS	SOURCE
1	Slope	Cartosat DEM
2	Aspect	Cartosat DEM
3	Elevation	Cartosat DEM
4	Lineament density	Bhuvan data set
5	Land use land cover	LANDSAT 8 Image
6	NDVI	LANDSAT 8 Image
7	Distance from road network	Google earth
8	Distance from drainage network	SOI Toposheet
9	Drainage density	SOI Toposheet
10	Distance from lineament	Bhuvan data set
11	Geology	SOI Toposheet
12	Soil	SOI Toposheet
13	Rainfall density	IMD rainfall data

Identification of potential landslide zones requires the systematic organization of causative factors based on their relative significance. This was achieved through a rating scheme that assigns numerical values to factors and their individual classes. The scheme was developed using insights from field observations and established knowledge on landslide-conditioning parameters (Ghorai et al., 2015; Pareta et al., 2012; Rawat et al., 2015; Sarkar & Kanungo, 2004). In the present study, each factor was assigned an inverse numerical ranking on a five-point scale (1–5), with higher values corresponding to greater influence on slope instability. Similarly, classes within each thematic layer were assigned weights reflecting their relative contribution to landslide occurrence.

All thematic layers were integrated using the Weighted Overlay Method (WOM) available in ArcGIS. The weighted overlay computation follows Eq. (1):

$$S=\Sigma Wi\ Sij/\Sigma Wi \qquad (Eq.1)$$

Where, Wi is the weight i^{th} factor map, Sij is the ith spatial class weight of jth factor map, S is the spatial unit value in output map.

Weighted overlay analysis offers a straightforward and robust framework for evaluating landslide susceptibility (Erener & Uzgeun, 2008; Bachri & Shresta, 2010; Intarawichian & Dasananda, 2010; Ahmed & Rogers, 2014). In total, thirteen environmental factors were utilized to generate the susceptibility map. All factor layers were standardized to a common scale (1–5) prior to integration.

The resulting landslide hazard zonation (LHZ) map was categorized into five classes: stable, moderately stable, moderately unstable, highly unstable, and critical zones. Validation of the LHZ map was performed using a landslide inventory compiled from historical records and field investigations. Ground truth points, including paleo-landslide locations, were collected using handheld GPS units and overlaid on the hazard map to assess its predictive reliability.

3. Result and Discussion

3.1 Landslide Conditioning Parameters and Thematic Layers

In the present investigation, landslide hazard zonation for Nilambur Taluk was carried out using thirteen conditioning parameters: slope, elevation, drainage density, rainfall, lineament density, aspect, land use/land cover (LULC), geology, soil, distance from drainage, distance from lineaments, distance from road networks, and NDVI. A brief description of each parameter and the corresponding thematic layers is provided below.

3.2 Slope

Slope is one of the most critical factors influencing slope stability in landslide hazard studies. The slope map was derived from ASTER DEM with a 30 m interval. Steeper slopes facilitate rapid runoff and reduce infiltration, thereby increasing susceptibility to failure, while gentle slopes allow greater infiltration and reduced shear stress (Lee & Sambath, 2006). In the study area, slope values range from 0° to >72°, classified into five categories (<5°, 5–10°, 10–15°, 15–25°, >25°) (Table 2; Fig. 2). Higher slopes are mainly concentrated in the eastern, northwestern, and southeastern regions.

3.3 Aspect

Aspect exerts significant control on microclimatic conditions that influence landslide initiation, such as solar radiation, wind exposure, rainfall distribution, and soil moisture (Liu et al., 2024; Tehulie et al., 2021). Aspect was extracted from the DEM and classified into nine categories, including flat. Maximum ranks were assigned to south-, southwest-, and west-facing slopes (Table 2; Fig. 3), which are considered more susceptible to instability.

Table 2. Assignment of ranking and weightage values of different thematic layers

Sl.No	Parameters	Classes	Rank	Weightage (%)
1	Slope (Degrees)	0 – 5	1	15
		5 – 10	2	
		10 – 15	3	
		15 – 25	4	
		25<	5	
2	Aspect	Flat	1	12
		North	1	
		North East	2	
		East	3	
		South East	3	
		South	5	
		South West	4	
		West	4	
		North West	2	
3	Drainage Density	0 – 1.2	1	10
		1.2 – 2.4	2	
		2.4 – 3.6	3	
		3.6 – 4.8	4	
		4 .8 – 6	5	
4	NDVI	-0.13 – 0.12	5	8
		0.12 – 0.22	4	
		0.22 – 0.32	3	
		0.32 – 0.42	2	
		0.42 – 0.62	1	
5	Geology	Hornblende Biotite Gneiss	3	5
		Charnokite, Hornblende Biotite Schist, Magnetite Quartzite, Talc Garnet Schist	4	
		Laterite	5	
6	Rainfall	2130 – 2649	3	10
		2649 – 3197	4	
		3197 - 3510	5	
7	Distance to the road networks	0 – 50	5	5
		50 – 100	4	
		100 – 150	3	
		150 – 200	2	
		200 <	1	
8	Distance to the Drainage networks	0 – 50	5	5
		50 – 100	4	
		100 – 150	3	
		150 – 200	2	
		200 <	1	
9	Distance to the Lineaments	0 – 50	5	5
		50 – 100	4	
		100 – 150	3	
		150 – 200	2	
		200 <	1	

10	Lineament density	0 – 0.3	1	5
		0.3 – 0.6	2	
		0.6 – 0.9	3	
		0.9 - 1.2	4	
		1.2 – 1.4	5	
11	Land use /Landcover	Paddy	1	10
		Water Body, Barren Rock	2	
		Forest Land	3	
		Mixed Vegetation	4	
		Rubber Plantation	5	
12	Soil	Very deep well drained Gravelly clay soil, Clay soil and Loamy Soil	3	5
		Deep and well drained Gravelly Soil	4	
		Shallow Gravelly soil	5	
13	Elevation	0 – 250	1	5
		250 – 500	2	
		500 – 750	3	
		750 – 1000	4	
		1000<	5	

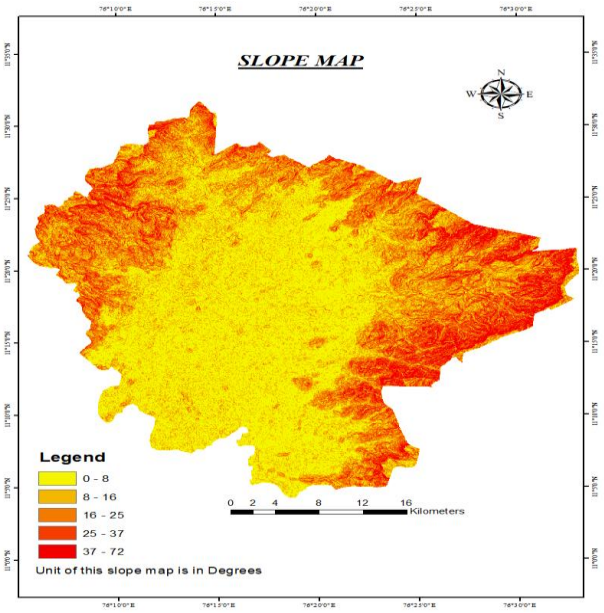

Figure 2. Landslide factor map of slope

3.4 Drainage Density

Drainage density reflects the degree of dissection and erosional intensity of terrain, thus serving as an important indicator of slope instability. Higher drainage density commonly corresponds to younger, more dynamic landscapes prone to erosion and mass movement (Liu et al., 2024). Drainage density in the study area ranges from 0–6 km/km^2 and was classified into five categories (Table 2; Fig. 4). Areas with higher drainage density exhibit greater landslide susceptibility.

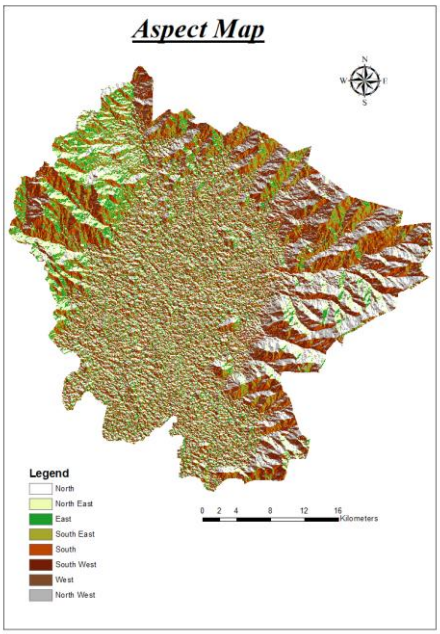

Figure 3. Landslide factor map of aspect

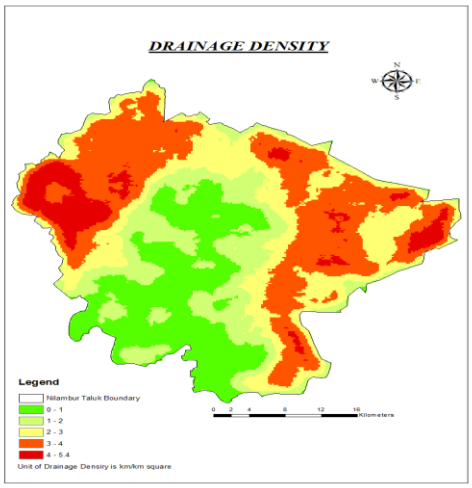

Figure 4. Landslide factor map of drainage density

Normalized Difference Vegetation Index (NDVI)

The NDVI layer was generated from Landsat 8 imagery. Vegetation cover enhances slope stability by increasing root cohesion and reducing pore-water pressure through evapotranspiration. Conversely, sparsely vegetated or barren areas are more prone to erosion and failure. Reduction in vegetation cover due to land-use change significantly elevates landslide risk (Ebrahim et al., 2019). Higher NDVI values represent stable, well-vegetated areas.

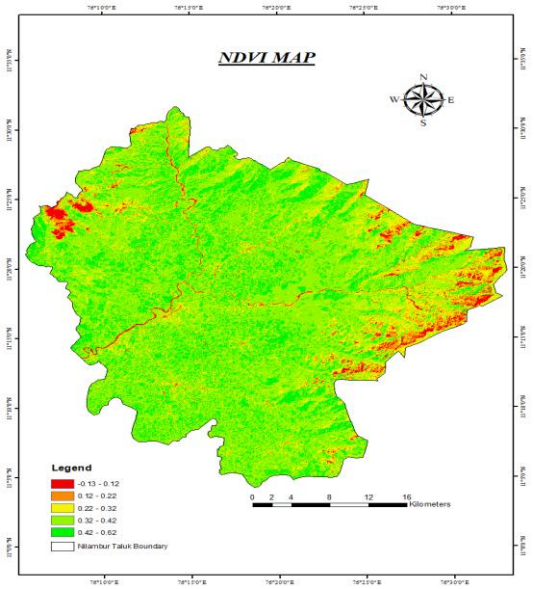

Figure 5. Landslide factor map of NDVI

3.5 Geology

The geological map (Fig. 6) reveals that the study area comprises hornblende–biotite gneiss, charnockite, schists, magnetite quartzite, talc–garnet schist, and laterite. Laterites and hornblende–biotite gneiss are particularly susceptible to slope failure (Anoop, 2013). Six lithological categories were delineated, with respective rankings assigned based on susceptibility (Table 2; Fig. 7).

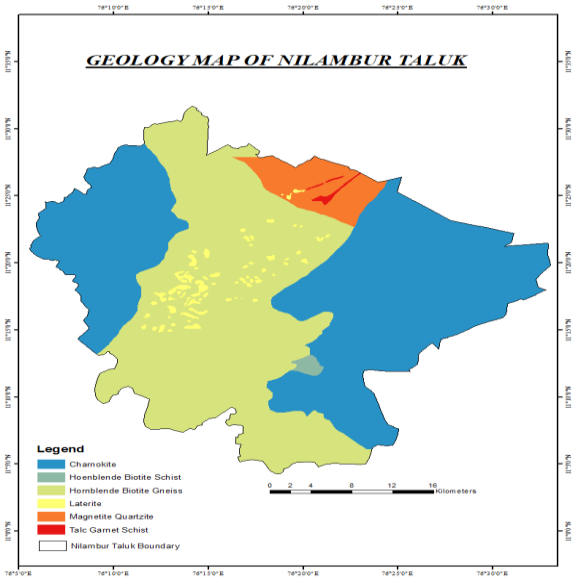

Figure 6. Landslide factor map of Geology

3.6 Rainfall

Rainfall is the dominant triggering factor for landslides in Nilambur Taluk. Continuous heavy rainfall promotes infiltration and elevates pore-water pressure,

resulting in slope failure. IMD rainfall data were used to generate the rainfall density map using the IDW method. Rainfall intensity ranges from 2130–3510 mm and is grouped into three classes (Table 2; Fig. 7). Regions receiving >2000 mm annually, especially at higher elevations, exhibit elevated susceptibility (Kuriakose et al., 2009).

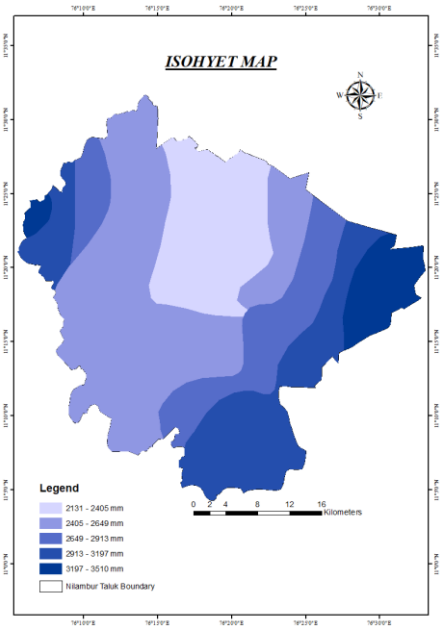

Figure 7. Landslide triggering factor map of Rainfall

3.7 Distance to Road Networks

Road construction in steep terrains often involves slope excavation, which creates discontinuities and destabilizes slopes, increasing landslide risk (Ebrahim et al., 2019). Distances to roads were categorized into five classes (0–50, 50–100, 100–150, 150–200, >200 m) (Table 2; Fig. 8). Maximum weightage was assigned to areas within 50 m of roads.

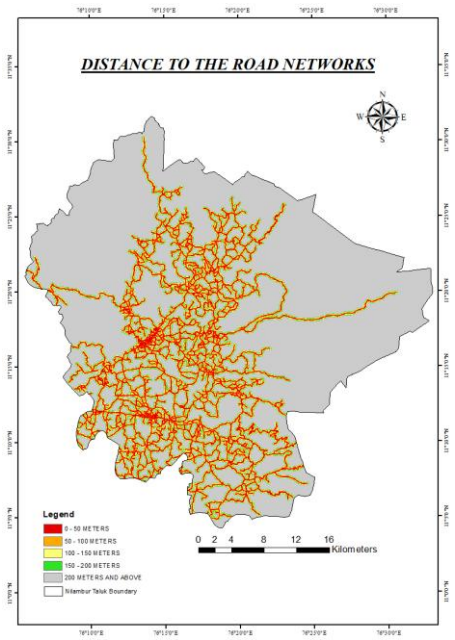

Figure 8. Landslide factor map of distance to the road networks

3.8 Distance to Drainage

Proximity to drainage channels significantly influences slope stability due to toe erosion and increased saturation (Qiu et al., 2025). Five distance classes were generated (0–50 to >200 m) (Table 2; Fig. 9). Areas closest to drainage (<50 m) are most susceptible.

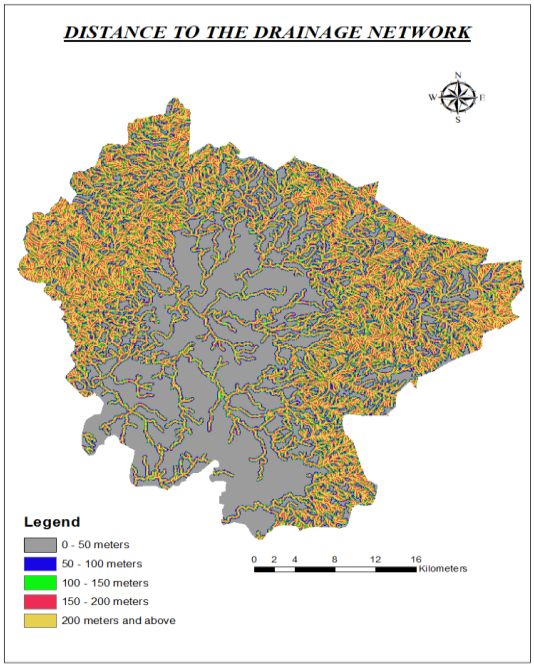

Figure 9. Landslide factor map of distance to drainage networks

3.9 Distance to Lineaments

Lineaments represent structural discontinuities that facilitate infiltration and weakening of slope materials. Distances to lineaments were classified into five categories (Table 2; Fig. 10). Areas within 50 m of lineaments show higher landslide incidence.

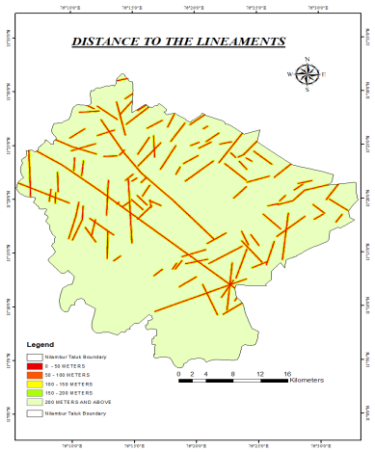

Figure 10. Landslide factor map of distance to the lineaments

3.10 Lineament Density

Lineament density was extracted from Bhuvan imagery. Areas of high lineament density correspond to zones of structural weakness and higher susceptibility to slope failure. Five classes were defined (0–1.4 km/km^2) (Table 2; Fig. 11).

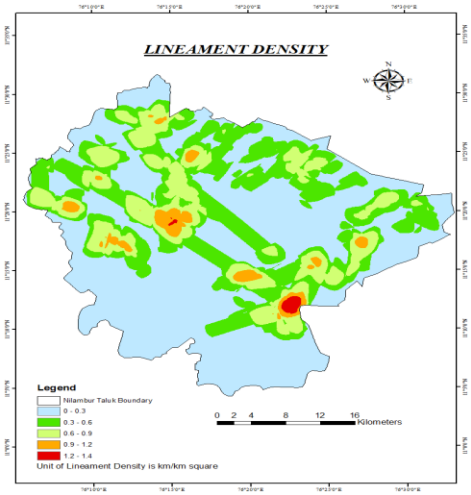

Figure 11. Landslide factor map of lineament density

3.11 Land Use/Land Cover (LULC)

LULC was derived from Landsat 8 imagery using supervised classification. The study area is characterized by six classes: paddy fields, water bodies, barren rock, forest land, mixed vegetation, and rubber plantations (Table 2; Fig. 12). Rubber plantations and barren areas (rank 5) show higher susceptibility due to reduced root cohesion and anthropogenic disturbance.

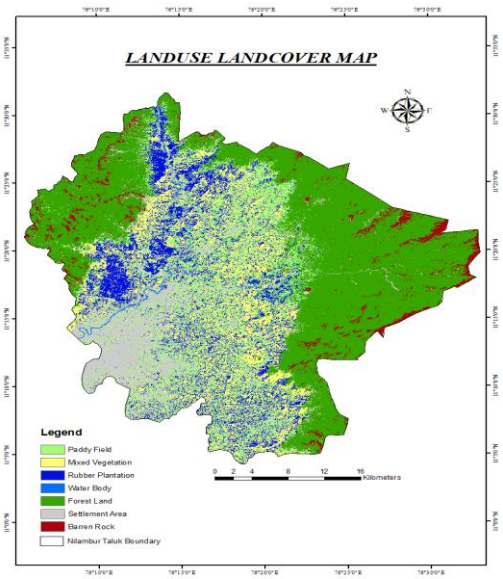

Figure 12. Landslide factor map of Landuse/Land cover

3.12 Soil

Soil thickness and type significantly influence slope stability. The study area includes very deep well-drained gravelly clay, clay and loamy soils, deep well-drained gravelly soils, and shallow gravelly soils (Table 2; Fig. 13). Shallow and gravelly soils are more prone to failure (Asla. K, 2014).

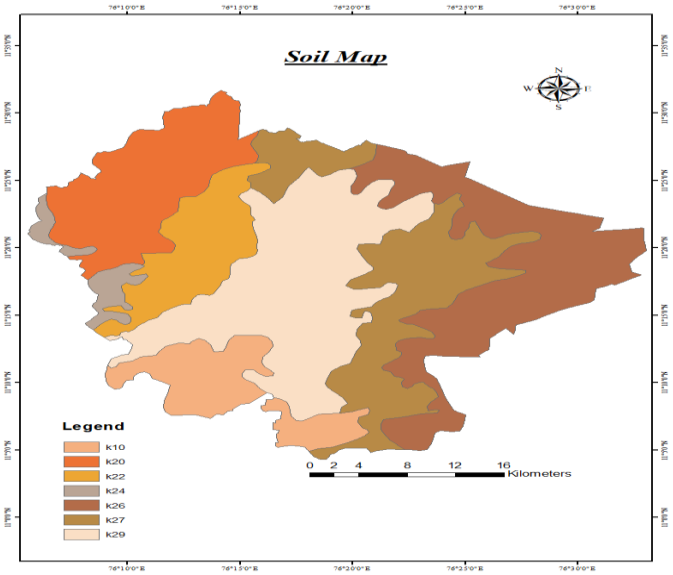

Figure 13. Landslide factor map of soils

3.13 Elevation

Elevation was extracted from SRTM DEM. Landslide susceptibility increases with elevation due to steeper terrain and thinner soil cover (Ajin et al., 2014). Five elevation classes were defined (>250 to >1000 m) (Table 2; Fig. 14). Higher elevations in the east and northwest exhibit maximum susceptibility.

3.14 Potential Landslide Hazard Zonation (LHZ)

Weighted Overlay Index (WOI) analysis was performed using an inverse ranking scheme. Thirteen thematic layers were integrated to generate the LHZ map, classified into five classes: Critical Zone (CZ), Highly Unstable Zone (HUZ), Moderately Unstable Zone (MUZ), Moderately Stable Zone (MSZ), and Stable Zone (SZ) (Table 3; Fig. 15). Results indicate that: 2.62% of the area falls under the Critical Zone, 16.43% under Highly Unstable Zone, 39.69% under Moderately Unstable Zone, 33.82% under Moderately Stable Zone and 7.3% under Stable Zone.

Approximately 266.23 km^2 exhibits high to very high landslide hazard. High-susceptibility zones occur mainly in the northwest and southeast. Slope (>25°), aspect, rainfall, geology, and drainage density exert dominant control over instability.

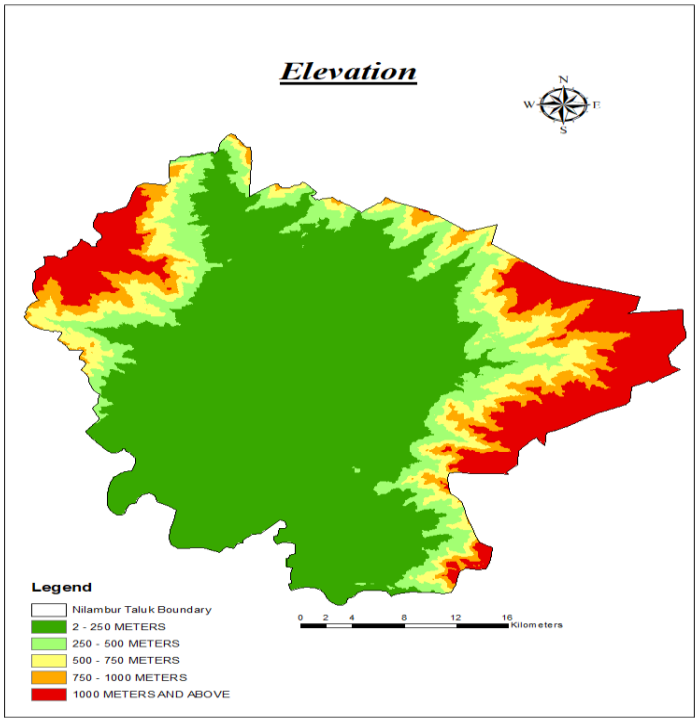

Figure 14. Landslide factor map of Elevation

3.15 Landslide Inventory and Validation

Validation was performed using 46 paleo-landslide locations obtained from the Geological Survey of India and the Kerala landslide inventory (Cobos-Mora et al., 2023). Ground verification was also conducted. Results show that: 46.8% of historical landslides fall within the Critical and Highly Unstable Zones, 42.55% fall within 100 m of these zones and 10.63% occur within 500 m, demonstrating strong agreement between the LHZ map and historical events (Fig.16).

Table 3. Percentage of area in the different category of Landslide hazard zonation

Sl.No	Category	Area (Sq.Km)	Area (%)
1	Stable	103.79	7.43
2	Moderately Stable	472.68	33.82
3	Moderately Unstable	554.69	39.69
4	Highly Unstable	229.56	16.43
5	Critical	36.67	2.62

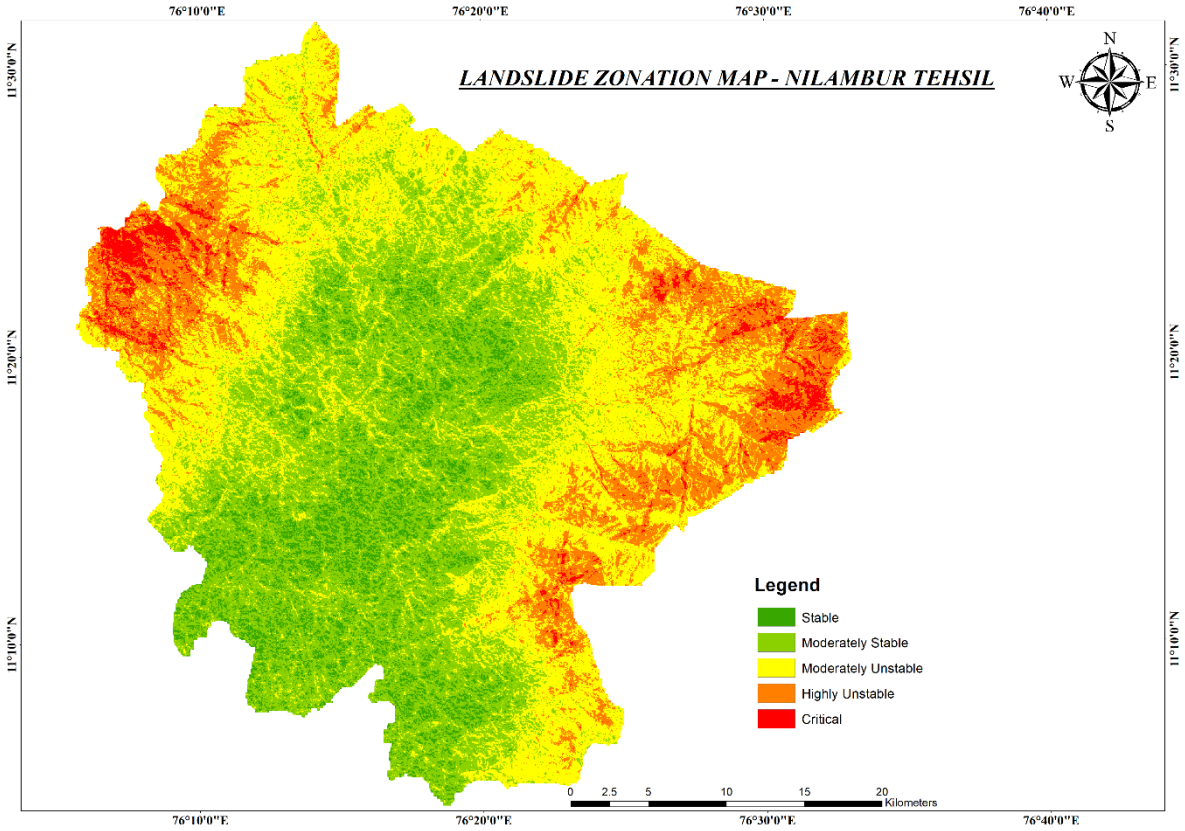

Figure 15. Landslide Hazard Zonation Map of Nilambur Taluk

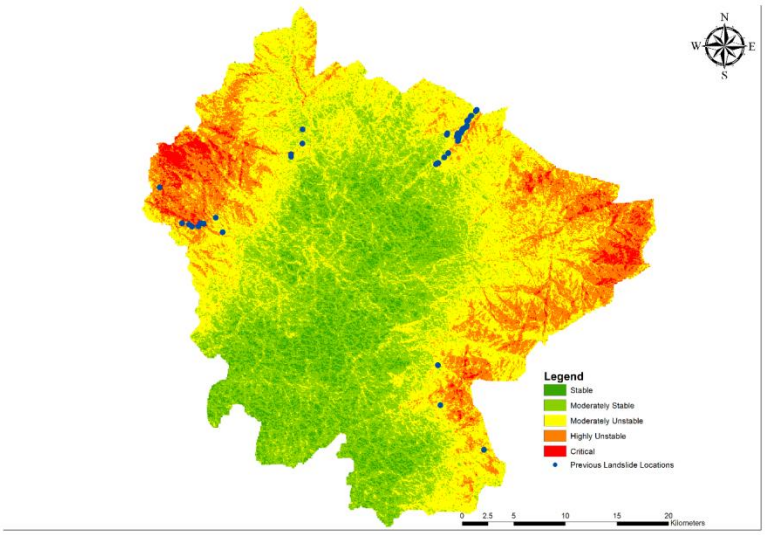

Figure.16. Landslide inventory and validation of Nilambur Taluk

4. Limitations and Future Directions

This study, while providing a robust landslide hazard zonation framework for Nilambur Taluk, is subject to several limitations that should be acknowledged. The weighted overlay method relies on expert-based assignment of weights and ranks, which introduces a degree of subjectivity and may influence the final hazard classification.

Additionally, the use of medium-resolution datasets such as Landsat imagery and DEM (30 m) may not fully capture fine-scale terrain variability and localized slope instability processes. The landslide inventory used for validation, although useful, is relatively limited in size and may not represent all historical events, potentially affecting model accuracy. Temporal variability, particularly short-term extreme rainfall events and land-use changes, is not dynamically incorporated into the model, which constrains its predictive capability under changing environmental conditions. Future research should focus on integrating higher-resolution datasets (e.g., LiDAR), employing advanced machine learning or hybrid modeling techniques, and developing time-series-based susceptibility assessments that account for climate variability and anthropogenic influences. Expanding and updating the landslide inventory database through continuous monitoring and incorporating real-time geospatial data would further enhance the reliability and applicability of landslide hazard assessments for sustainable land-use planning and disaster risk reduction.

5. Conclusion

This study successfully achieved its primary objective of delineating landslide hazard zones in Nilambur Taluk using a GIS-based weighted overlay approach integrating thirteen conditioning parameters derived from remote sensing and geospatial datasets. The resulting Landslide Hazard Zonation (LHZ) map classified the region into five categories ranging from stable to critical hazard zones, providing a spatially explicit assessment of landslide susceptibility across the study area. The model results indicate that approximately 19.05% of the area falls within highly unstable and critical zones, which are predominantly associated with steep slopes, intense rainfall, high drainage density, and structurally weak lithological units.

Model validation using 46 historical landslide locations demonstrated strong agreement between the predicted hazard zones and observed landslide occurrences. Specifically, 46.8% of the inventoried landslides fall within the Critical and Highly Unstable zones, while 42.55% occur within 100 m of these zones, indicating that the model effectively captures the spatial pattern of landslide susceptibility in the region. These findings confirm the reliability of the proposed approach for regional-scale hazard assessment and highlight the usefulness of the generated LHZ map as a decision-support tool for land-use planning, infrastructure development, and disaster risk reduction in Nilambur Taluk.

Declaration of Generative AI and AI-Assisted Technologies in the Writing Process

ChatGPT as an AI-assisted tool for language refinement, grammar checking , and improving the clarity of scientific writing. The use of this tool was limited to supporting the writing process and did not involve the generation of original research content, data analysis, or interpretation of results. After using this tool, the authors carefully reviewed, revised, and ensured the accuracy and integrity of the manuscript. The author(s) take full responsibility for the content of this publication.

Authorship Contribution Statement

Arunkumar K.S contributed to conceptualization, methodology, supervision, formal analysis, and writing the original draft. Mufeeda C.T as a student researcher, was primarily responsible for field investigation, data collection, and data curation, as well as contributing to the initial draft preparation.

Declaration of Competing Interest

The authors declare that they have no known competing financial interests or personal relationships that could have appeared to influence the work reported in this paper.

References

Ahmed, M. F., & Rogers, J. D. (2014). A regional level preliminary landslide susceptibility study of the upper Indus river basin. *Euro J Remote Sensing*, *47*, 343–373.

Ajin, R. S., Vinod, P. G., & Menon, A. R. R. (2014). *Landslide hazard zonation using RS and GIS technique: a case study of Meenachil and Kanjirappally Taluk, Kottayam District, Kerala, India*.

Amrutha, A. S., Jothika, M., Athira, A., Pradeep, G. S., & Nandu, M. R. (2026). From slopes to streams: Geospatial characterization of landslide dynamics and downstream impacts in the Western Ghats highland panchayats, Kerala, India. *International Journal of Disaster Studies and Climate Resilience*, *2*(1), 81. https://doi.org/10.64866/j.ijdscr.2026.10025

Anoop, K. G. (2013). *Assessment and prediction of shallow Landslide susceptibility of Udumbanchola and Devikulam taluks in Idukki district,Kerala through analytical hierarchy process*.

Asla. K. (2014). *Landslide hazard zonation of Nilambur taluk using remote sensing*.

Bachri, S., & Shresta, R. P. (2010). Landslide hazard assessment using analytic hierarchy processing (AHP) and geomorphic information system in Kaligrsing area of Central Java Province Indonesia. *5th Annual International Workshop and Expo on Sumatra Tsunami Disaster and Recovery*, 107–112.

Badapalli, P. K., Nakkala, A. B., Kottala, R. B., Gugulothu, S., Hasher, F. F. Ben, Mishra, V. N., & Zhran, M. (2025). Landslide Susceptibility Level Mapping in Kozhikode, Kerala, Using Machine Learning-Based Random Forest, Remote Sensing, and GIS Techniques. *Land*, *14*(7), 1453. https://doi.org/10.3390/land14071453

Chen, Z., & Wang, J. (2007). Landslide hazard mapping using logistic regression model in Mackenzie Valley. *Canada. Nat. Haz.*, *42*, 75–89.

Cobos-Mora, S. L., Rodriguez-Galiano, V., & Lima, A. (2023). Analysis of landslide explicative factors and susceptibility mapping in an andean context: The case of Azuay province (Ecuador). *Heliyon*, *9*(9), e20170. https://doi.org/10.1016/j.heliyon.2023.e20170

Doukanari, M., Tzouvaras, M., Fotiou, K., Stylianou, N., Mettas, C., & Hadjimitsis, D. (2025). A GIS-based multi-criteria decision analysis framework for landslide risk assessment: a case study in Amathounta, Limassol, Cyprus. In I. Gitas, A. Anayiotos, V. Ambrosia, N. Kyriakides, G. Papadavid, K. Themistocleous, S. C. Michaelides, D. G. Hadjimitsis, A. Christofi, C. Danezis, & F. Schwandner (Eds.), *Eleventh International Conference on Remote Sensing and Geoinformation of the Environment (RSCy2025)* (p. 81). SPIE. https://doi.org/10.1117/12.3075513

Ebrahim, N., Meisa, M., & Samira, S. (2019). *Landslide susceptibility mapping using different GIS based bivariate models*.

Erener, A., & Uzgeun, H. S. B. D. (2008). Analysis on landslide hazard mapping methods: regression models versus weight rating. *The International Archives of the Photogrammetry, Remote Sensing and Spatial Sciences, Vol. 37 (Part B8)*.

Froude, M. J., & Petley, D. N. (2018). Global fatal landslide occurrence from 2004 to 2016. *Nat. Hazards Earth Syst. Sci.*, 2161–2181.

Ghorai, D., Maiti, S., & Paul, A. K. (2015). Landslide susceptibility mapping: a case study of cauvery basin and east flowing rivers south of cauvery basin. *India. J Remote Sensing GIS*, *6*(1), 24–36.

Gunnell, Y., & Fleitout, L. (2000). *Morphotectonic Evolution of the Western Ghats, India in "Geomorphology and global tectonics"* (M. A. Summerfield, Ed.). Wiley.

Intarawichian, N., & Dasananda, S. (2010). Analytical hierarchy process for landslide susceptibility mapping in lower Mae Cheam watershed, Northern Thailand. *Suranaree J. Sci. Technol.*, *17*(3), 277–292.

Jishnusachidanandhan, & Ajith, J. (2015). *Identification of potential Landslide vulnerable zones of Wayanad District, Kerala using remote sensing and GIS*.

Kuriakose, S. L., Sankar, G., & Muraleedharan, C. (2009). History of landslide susceptibility and a chorology of landslide-prone areas in the Western Ghats of Kerala, India. *Environmental Geology*, *57*(7), 1553–1568.

Lee, S., & Sambath, T. (2006). Landslide susceptibility mapping in the DamreiRomel area, Cambodia using frequency ratio and logistic regression models. *Envir. Geol.*, *50*, 847–855.

Liu, S., van Meerveld, I., Zhao, Y., Wang, Y., & Kirchner, J. W. (2024). Seasonal dynamics and spatial patterns of soil moisture in a loess catchment. *Hydrology and Earth System Sciences*, *28*(1), 205–216. https://doi.org/10.5194/hess-28-205-2024

Martha, T., Roy, P., Khanna, K., Kotteeswaran, M., & Vinod Kumar, K. (2019). Landslides Mapped using Satellite Data in the Western Ghats of India After Excess Rainfall During August 2018. *Current Science*, *117*, 804–812.

Md. Motiur Rahman, Md. Toriqul Islam, & Mst. Esrat Jahan. (2025). Climate Change Perception of Farmers and Its Effect on the Technical Efficiency of Rice Production. *Indonesian Journal of Sustainable Agriculture and Environmental Sciences (IJSAES)*, *1*(2), 64–77. https://doi.org/10.65896/ijsaes.v1i2.15

Nima, Z., SHINU, N., S., A., A.S., Y. S., & A.V. Panicker, A. (2025). Assessment of Groundwater Quality Along the Coastal Aquifers of Kollam Corporation, Southern Kerala, India. *Indonesian Journal of Sustainable Agriculture and Environmental Sciences (IJSAES)*, *1*(2), 55–63. https://doi.org/10.65896/ijsaes.v1i2.12

Olade, M. A. (2025). Geology and Mineral Deposits of Ondo State, Southwestern Nigeria: Assessment of Potential Benefits of Resource Exploitation. *Journal of Scientific Research and Reports*, *31*(11), 459–483. https://doi.org/10.9734/jsrr/2025/v31i113681

Pareta, K., Kumar, J., & Pareta, U. (2012). Landslide hazard zonation using quantitative methods in GIS. *Int. J. Geospatial Eng. Technol.* , *1*, 1–9.

Pichamuthu, C. S. (1976). Some Problems Pertaining to The Peninsular Gneissic Complex. *Journal Geological Society of India*, *17*(1), 1–16. https://doi.org/10.17491/jgsi/1976/170101

Prasannakumar, V., & Vijith, H. (2012). Evaluation and validation of landslide spatial susceptibility in the Western Ghats of Kerala, through GIS-based Weights of Evidence model and area under curve technique. *Journal of the Geological Society of India* , *80*(4), 515–523.

Qiu, E., Qin, S., Li, C., Liu, J., Zhong, C., Wang, H., Xu, D., & Hao, S. (2025). Analysis of the rainfall-triggering mechanism and movement characteristics of debris flows in the southwest mountainous area. *Physics of Fluids*, *37*(10). https://doi.org/10.1063/5.0287454

Rawat, M. S., Uniyal, D. P., Dobhal, R., Joshi, V., Rawat, B. S., Bartwal, A., Singh, D., & Aswal, A. (2015). Study of landslide hazard zonation in Mandakini Valley, Rudraprayag district, Uttarakhand using remote sensing and GIS. *Current Science*, *109*(1), 158–170.

Sarkar, S., & Kanungo, D. P. (2004). An integrated approach for landslide susceptibility mapping using remote sensing and GIS. *Photogram Eng. Remote Sens.*, *70*(5), 617–625.

Shafi, A., & Khan, A. (2025). Air to Soil Temperature Comparison: A Case Study for Tarnab, Pakistan. *Indonesian Journal of Sustainable Agriculture and Environmental Sciences (IJSAES)*, *1*(3), 112–119. https://doi.org/10.65896/ijsaes.v1i3.17

Sreekumar, S., & Arish, A. (2017). Geospatial Approach for Landslide Disaster Management: A Case Study from India. *International Journal of Applied and Advanced Scientific Research*, *2*(2), 120–127.

Tehulie, N. S., Fikadu, T., & Purba, J. H. (2021). Response of Mungbean [Vigna radiata (L.)Wilczek] Varieties to Plant Spacing under Irrigation at Gewane, Northeastern Ethiopia. *Agro Bali: Agricultural Journal*, *4*(1), 1–14. https://doi.org/10.37637/ab.v0i0.613